JGR Biogeosciences

RESEARCH ARTICLE
10.1029/2025JG009168

Organic Carbon Burial Rates in Muddy Temperate Shelf Sea Sediments

Hannah C. Muir[1,2], David G. Reading[3], Phillip E. Warwick[3], James A. Strong[2], Kate Peel[2], Rowan Henthorn[4], Jacqui Keenan[4], Peter F. Duncan[4], Jan G. Hiddink[5], Martin W. Skov[5], Richard K. F. Unsworth[1], and Claire Evans[2]

[1]School of Biosciences, Swansea University, Swansea, UK, [2]Ocean Biogeosciences, National Oceanography Centre, Southampton, UK, [3]GAU-Radioanalytical Laboratories, School of Ocean and Earth Science, University of Southampton, National Oceanography Centre, Southampton, UK, [4]Department of Environment, Food and Agriculture (DEFA), Isle of Man Government, St John's, Isle of Man, [5]School of Ocean Sciences, Bangor University, Anglesey, UK

Key Points:

- Organic carbon burial estimates are improved by empirical depth- and age-resolved sedimentary analyses
- Approx. 53%–91% of organic carbon accumulated in the first decade remains buried for over 100 years in the Western Irish Sea Mud Belt
- Organic carbon accumulation and burial rates are higher in muddier sediments than in sandier sediments

Supporting Information:

Supporting Information may be found in the online version of this article.

Correspondence to:

H. C. Muir,
hmuir@noc.ac.uk

Citation:

Muir, H. C., Reading, D. G., Warwick, P. E., Strong, J. A., Peel, K., Henthorn, R., et al. (2026). Organic carbon burial rates in muddy temperate shelf sea sediments. *Journal of Geophysical Research: Biogeosciences*, *131*, e2025JG009168. https://doi.org/10.1029/2025JG009168

Received 2 SEP 2025
Accepted 16 FEB 2026

Abstract Muddy continental shelf sediments act as important sinks for atmospheric CO_2 by accumulating organic matter, a small fraction of which is buried and stored as organic carbon (OC) over long timescales. Quantifying long-term OC burial in shelf sediments is critical for understanding their role in climate regulation; however, this remains difficult due to limited age-resolved data and the challenges of determining sediment accumulation rates and temporal changes in OC content. To address this, we quantified age-resolved OC storage over the past two centuries in the upper 50 cm of the Western Irish Sea Mud Belt (WISMB) by measuring depth-resolved OC content and sediment accumulation rates. The OC content (0.15%–1.62%), OC storage (1.30–15.15 gC cm^{-3}), and sediment accumulation rates (0.26–0.37 cm yr^{-1}) vary both spatially and temporally, with the highest OC accumulation and burial occurring in muddier, deeper-water sediments. Between 53% and 91% of the OC accumulated in the surface 2 cm over the past 8 years (17.09–39.47 gC m^{-2} yr^{-1}), and 60%–68% of the OC accumulated in the upper 10 cm over the past 38 years (21.90–51.13 gC m^{-2} yr^{-1}), remains buried for more than 100 years (14.03–33.50 gC m^{-2} yr^{-1}). These rates are comparable to those reported for other muddy continental shelf regions, including mud patches, coastal fjords, and glacial troughs.

Plain Language Summary Muddy continental shelves help regulate the climate by capturing and storing organic matter that settles on the seabed. While most organic carbon (OC) is released back into the environment, a small amount becomes buried in the sediment, contributing to long-term OC storage. Understanding how much OC is buried over time is important for estimating the role of shelf seas in climate regulation. This is challenging because it requires knowing sediment age and how much OC the seabed stores. To address this, we measured OC storage in younger surface sediments and older deeper sediments in the Western Irish Sea Mud Belt (WISMB), a muddy depositional zone in the Irish Sea. We found that the amount of OC stored and the rate of sediment accumulation varied across the region, despite its relatively small size. About three-quarters of OC accumulated over the past decade and two-thirds of OC accumulated over the past four decades remains buried up to 200 years, particularly in muddier sediments. The amount of OC stored is similar to other muddy areas, such as mud patches, coastal fjords, and glacial troughs, highlighting the important role of continental shelf areas such as the WISMB in storing OC and helping to regulate the climate.

1. Introduction

Continental shelf sediments are an important component of the global carbon cycle, acting as a significant sink for atmospheric CO_2 absorbed by the ocean (Atwood et al., 2020). This role is particularly notable in muddy sediment deposits, such as coastal fjords, mud patches, and glacial troughs (Diesing et al., 2024; Dubosq et al., 2021; Smeaton, Hunt, et al., 2021). Photosynthetic marine organisms assimilate CO_2 from the atmosphere and water column, converting inorganic carbon (IC) to organic carbon (OC; Mathis et al., 2024). More than 95% of OC undergo aerobic and anaerobic remineralization before burial within sediments (Chen et al., 2022; de Haas et al., 2002). As burial proceeds, reactive labile OC is degraded, leaving more refractory OC behind (Burdige, 2007). This OC degradation can be accelerated by repeated oxic–anoxic transitions driven by sediment resuspension and mixing from bioturbation, hydrodynamics (waves, tides, storms) and anthropogenic activities such as bottom trawling, which are widespread on continental shelves (Aller, 1994; Song et al., 2022; van de Velde et al., 2018).

OC accumulation rates (OCARs) and OC burial rates (OCBRs) are key metrics for quantifying the capacity of coastal and marine sediments to draw down atmospheric CO_2 over short-term (decadal) and long-term (centennial to millennial) timescales, respectively (Kristensen et al., 2025). As it has been proposed that durable CO_2 removal for achieving net-zero targets should exceed 1,000 years (Brunner et al., 2024), distinguishing between OCARs and OCBRs is essential to avoid overestimating the long-term climate change mitigation and adaptation potential of marine sediments (Williamson & Gattuso, 2022). However, inconsistent definitions and non-standardized methodologies have led to misleading conclusions and poor comparability between studies (Wilkinson et al., 2018). Terms such as OC flux, accumulation, sequestration, and burial are often used interchangeably to describe both short-term accumulation and long-term burial processes (Hu et al., 2016), underscoring the need for clear terminology linked to explicit timescales.

A major challenge is that substantial OC degradation occurs near the sediment–water interface before stabilizing at depth (Burdige, 2007). However, OCBRs are often estimated from surface sediments or unspecified depths without accounting for sediment age or OC stability (Hu et al., 2016; Sanders et al., 2010). This can lead to misleading comparisons between sediment layers of different ages and overestimating their long-term OC burial potential (Wilkinson et al., 2018). Reliance on surface sediment samples is often due to the relative ease of obtaining grab samples and short sediment cores during routine monitoring, contrasted with limited data from deeper sediments (Dubosq et al., 2021; Graves et al., 2022). OC degradation rates also vary with depositional setting, sediment accumulation rate, and mineralogy, while temporal variability in OC supply further complicates assessments (Bradley et al., 2022; LaRowe et al., 2020). In addition, sediment mixing from bioturbation, hydrodynamics, and chronic bottom trawling can alter OC content and distort sediment accumulation rates, which can increase uncertainty in OCAR and OCBR estimates (Dubosq et al., 2021; Johannessen, 2023; Paradis et al., 2019; van de Velde et al., 2018; Wilkinson et al., 2018).

Studies in the Northeast Atlantic have begun to constrain OC accumulation and burial in muddy shelf environments, including mud patches (Dubosq et al., 2021), fjords (Smeaton, Yang, & Austin, 2021), and glacial troughs (Diesing et al., 2024). Building on this work, we present the first empirical OCAR and OCBR estimates for the Western Irish Sea Mud Belt (WISMB), which is predicted to be a major OC store in the Northeast Atlantic (Burrows et al., 2024; Smeaton, Hunt, et al., 2021). The WISMB is characterized by low tidal currents, low bed stress, and a seasonal gyre, all of which promote fine-grained sediment retention, with mud deposits up to 40 m thick (Belderson, 1964; Coughlan et al., 2015, 2021; Kershaw, 1986; Ward et al., 2025). Cyclonic tidal currents form a narrow tidal benthic boundary layer with minimal turbulence, facilitating deposition and reducing resuspension (Williams et al., 2019). Seasonal stratification also reinforces sediment retention within the gyre (Hill et al., 1997). The dominant OC source in the WISMB is phytoplankton, with production peaking in spring–summer during maximum light penetration and stratification, while zooplankton grazing drives significant remineralization (Burrows et al., 2024; Hill, 2007). Additional OC derives from allochthonous sources via water mass exchange with the Celtic Sea, Irish waters, and English waters (Bowers et al., 2013), as well as coastal vegetated habitats and terrestrial inputs from rivers (Burrows et al., 2024; O'Reilly et al., 2014).

To constrain sediment accumulation rates in the Irish Sea, natural and anthropogenic radionuclides can be used. The naturally occurring ^{210}Pb (22.3-year half-life) decays with depth, providing continuous dating (Appleby & Oldfield, 1978). Anthropogenic radionuclides such as ^{137}Cs (30-year half-life) and ^{241}Am (432.6-year half-life) are primarily derived from historical discharges from the Sellafield nuclear facility, notably a major 1975 release (Gray et al., 1995). These markers, when combined with ^{210}Pb profiles, can enable robust sediment accumulation rate estimates, of which there are only a few examples for the WISMB (Coughlan et al., 2015), facilitating OCAR and OCBR assessments. Here, we use these methods to quantify OCARs and OCBRs in the WISMB over the past two centuries, evaluate temporal and spatial changes in these rates, and assess the influence of sediment mixing processes on sedimentary OC dynamics in this naturally and anthropogenically disturbed seabed. These results advance our understanding of short- and long-term OC storage in muddy continental shelf sediments.

2. Materials and Methods

2.1. Sampling Site Selection

Sediments were sampled from the northeastern corner of the WISMB where permits were provided by the Isle of Man Government within their territorial sea. A total of 20 sampling stations were distributed across muddy sediments within the study region to ensure sediment samples were representative of the WISMB and to account

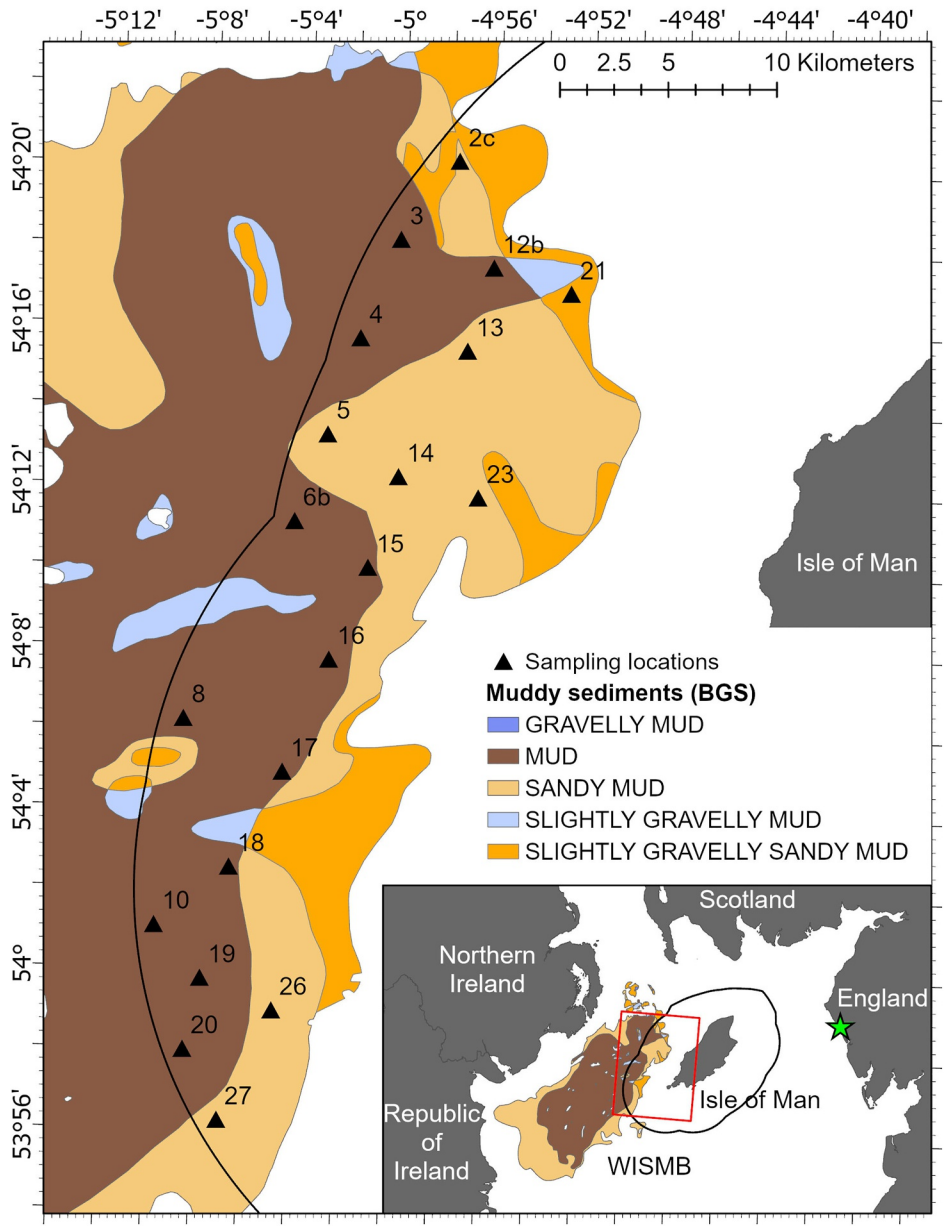

Figure 1. Map of the Western Irish Sea Mud Belt (WISMB) and sampling site locations labeled with sediment core identification codes (produced in ArcGIS Pro software). Colored areas show British Geological Survey seabed sediment classes for muddy sediments (mud (M), sandy mud (sM), gravelly mud and slightly gravelly mud ((g)M), and slightly gravelly sandy mud ((g)sM)) (250K data set; British Geological Survey, 2024). The inset map shows the WISMB in the Irish Sea relative to neighboring countries. The sampling region is highlighted by a red box. The Sellafield nuclear facility is marked with a green star on the west coast of England.

for spatial variability in sediment type and water depth at the edge of the WISMB. Sediment textural classifications informed the selection of muddy sediment sites (Figure 1; British Geological Survey, 2024; Folk, 1954), whereby sedimentary OC content is expected to increase with mud content. GEBCO Gridded Bathymetry Data (Figure S1 in Supporting Information S1; GEBCO Compilation Group, 2024) informed the selection of sites distributed across water depths of approximately 60–130 m (Table S1 in Supporting Information S1), to account for changes in tidal and current energy away from the edge of the WISMB. Increased energy at the seabed would be expected to reduce sediment accumulation rates and the proportion of finer sediments (e.g., mud), which would be expected to reduce OC content.

2.2. Sediment Sampling

Sediment cores were collected from 20 sites across the study area in June 2022 using a UWITEC gravity corer (height = 120 cm; internal diameter = 9 cm). Water depths at the sampling sites ranged from 66 to 132 m, which were recorded during corer deployment using the research vessel depth sounder and then corrected for tidal state. Overlying water was drained from the core liner after the sediment settled at the core surface to prevent loss of sediments resuspended during coring and to minimize sediment–water mixing during transport. The cores were stored upright at temperatures below 5°C to preserve their integrity and then transported upright to the National Oceanography Centre, Southampton, where all subsequent laboratory analyses were performed.

2.3. Sediment Core Processing

Sediment cores were split lengthwise using a Geotek core splitter at the British Ocean Sediment Core Research Facility (BOSCORF). High-resolution images of the smoothed sediment surfaces were captured using a Geotek Core Imaging System (MSCL-CIS) with a Geoscan V camera (1,000 pixels cm^{-1}). X-ray radiography images were collected for all sediment cores (except Sites 4, 8, 13, 14, 20, 2c, due to equipment failure) using a ScoutXcan Multi-Angle Digital 2D X-Ray System.

From one half of each split sediment core, sediment samples were taken from the center of the cores to minimize disturbance effects from coring. A U-channel of known volume was used to extract samples at depth intervals: every 2 cm for the top 20 cm of the sediment core, every 5 cm between 20 and 50 cm, and every 10 cm beyond 50 cm. Sampling resolution increased toward the sediment surface to account for more significant changes expected in sediment properties at shallower sediment depths (Howard et al., 2014). Samples were freeze-dried and homogenized, and both wet and dry weights were recorded before analysis.

These samples were subsequently analyzed for sediment dry bulk density (DBD), OC and total carbon content, and particle sizes. Analytical data were successfully collected from all samples up to 50 cm, except for Site 2c due to a dense shell layer at 48–50 cm. Average data sets used for sediment depth 45–50 cm thus excluded data for Site 2c.

2.4. Sediment Dry Bulk Density Analysis

Sediment DBDs were estimated using Equation 1.

Equation 1: Sediment dry bulk density (DBD) calculation.

$$\mathrm{DBD}\left(\mathrm{g\ cm^{-3}}\right) = \frac{\text{Mass of dry sediment (g)}}{\text{Original volume sampled (cm}^3\text{)}} \quad (1)$$

2.5. Elemental Analysis

The OC and total carbon contents, as well as stable carbon isotope ratios ($\delta^{13}C$), were measured using a Flash 2000 Elemental Analyzer (EA) coupled with a Delta V Advantage isotope ratio mass spectrometer (IRMS). To determine OC content, the IC was removed using 50% HCl and dried on a hot plate before analysis. Isotope data were reported in delta notation relative to the Vienna Pee Dee Belemnite (VPDB) standard.

Sediment OC density (SCD) was estimated using Equation 2.

Equation 2: Sediment organic carbon density (SCD) calculation.

$$\mathrm{SCD}\left(\mathrm{gC\ cm^{-3}}\right) = \frac{\text{OC content (\%)}}{100\%} * \mathrm{DBD}\left(\mathrm{g\ cm^{-3}}\right) \quad (2)$$

2.6. Particle Size Analysis

Particle size distributions were determined using a Malvern Mastersizer 3000 laser microgranulometer, following the NE Atlantic Marine Biological AQC Best Practice Guidance for Particle Size Analysis (PSA) (Mason, 2022). Every other sample depth was analyzed down to 40–45 cm (e.g., 0–2 cm, 4–6 cm, etc.), due to resource limitations. Samples were dispersed in a 1% Calgon solution (sodium hexametaphosphate) and sonicated for 10 min prior to analysis. Samples with particle diameters more than 2,000 μm were sieved using a 1,000 μm mesh prior to analysis, and the results from laser diffraction (volumetric) were scaled to the overall sample (mass) by assuming

constant sediment density. Particle size classes were grouped as clay (<3.9 μm), silt (3.9–62.5 μm), mud (<62.5 μm), and sand (62.5–2,000 μm) based on Udden (1914) and Wentworth (1922). The Folk (1954) classification scheme was used for sediment classification.

2.7. Radionuclide Analysis Using Gamma Spectrometry Measurements

The second half of 7 sediment cores (Sites 4, 8, 14, 15, 20, 21, 27) was sliced into 1 cm intervals throughout the upper 40 cm of sediment to produce higher resolution samples with sufficient volume for radionuclide analysis, which was used to estimate sediment accumulation rates. A portion of each sample within approximately 1 cm of the core liner was discarded to minimize disturbance/smearing effects from coring, and the remaining samples were freeze dried prior to analysis. These sites were selected arbitrarily from sampling stations across the study region that reflect the range of muddy sediment classifications and water depths in the northeast WISMB. Sediments were measured for ^{210}Pb, ^{137}Cs, and ^{241}Am using Mirion Canberra High Purity Germanium (HPGe) well-type gamma spectrometers (GAU-Radioanalytical, University of Southampton) under their accreditation to ISO/IEC17025. Data acquisition was performed using Genie-2000 (Mirion Canberra) and spectral analysis was performed using Fitzpeaks 32 deconvolution software. The HPGe detectors were efficiency calibrated using a certified, mixed gamma radionuclide standard (National Physical Laboratory, UK) which was homogenized into a near-identical sample matrix to that of the test sample. Samples were counted for 8 hr to achieve low limits of detection, achieving 10% precision.

2.8. Radionuclide Analysis Using Alpha Spectrometry Measurements

Alpha spectrometry (Ortec Octete) was conducted to measure the grand-daughter radionuclide, ^{210}Po, which would be in equilibrium with ^{210}Pb, for 3 sediment cores (Sites 4, 8, and 20) to cross-validate the ^{210}Pb activities, which were close to the instrumental limit of detection and had higher uncertainty. To prepare samples for alpha spectrometry, an aliquot of sample was spiked with ^{209}Po as a chemical yield monitor and then digested using *aqua regia*. A clean silver disc was then placed in the resultant digest for ^{210}Po autodeposition.

2.9. Estimation of Sediment Accumulation Rates

Average linear sediment accumulation rates were estimated from excess ^{210}Pb and excess ^{210}Po activities using the constant flux constant sedimentation (CF–CS) model (Appleby & Oldfield, 1978). These rates were derived from the sediment depth layers where the natural logarithm of the excess ^{210}Pb and excess ^{210}Po radionuclide activities decreased linearly with sediment depth, below the sediment mixed layer and above the supported ^{210}Pb and supported ^{210}Po (below ∼20 cm), where radionuclide activities are constant with sediment depth. These rates were validated using ^{137}Cs activity (impulse) peaks corresponding to the 1975 discharge maximum from the Sellafield nuclear facility relative to the core surface representing the year 2022, and the onset of cumulative ^{241}Am activities corresponding to ^{241}Am discharge records from the Sellafield nuclear facility (Gray et al., 1995). The ^{137}Cs radionuclide was used as an impulse marker due to its widespread dispersal throughout the Irish Sea as a Cs^{+} cation in seawater and weak sediment association, such that instantaneous deposition in the WISMB was assumed (Ray et al., 2020). While remobilization of ^{137}Cs may broaden the 1975 peak, the position of this subsurface maximum provides a reliable impulse marker. Meanwhile, the ^{241}Am radionuclide was used as an onset marker due to its high particle reactivity compared to ^{137}Cs and association with fine-grained sediments (e.g., mud patches), which can retain historic discharges in the local environment and provide a continuous supply of historic ^{241}Am throughout the WISMB, elevating sedimentary ^{241}Am activity concentrations (Ray et al., 2020). In addition, ^{241}Am can in-grow in situ through beta decay of ^{241}Pu. The high particle reactivity of ^{241}Am and the corresponding dominance of sediment transport processes rather than water circulation pathways for the distribution of the nuclide can result in a different lag time prior to deposition. However, this would not significantly impact core profiles given the sampling resolution relative to the accumulation rates in this study. Average linear sediment accumulation rates were therefore estimated from excess ^{210}Pb, excess ^{210}Po, and ^{137}Cs activity profiles, where reliable data were available, and validated using the ^{241}Am onset, to estimate sediment age for the top 50 cm.

2.10. Estimation of Organic Carbon Accumulation and Burial Rates

For the five sediment cores that were dated using radionuclide analysis, the sediment accumulation rates were used to define depths representing short-term OCARs at the sediment–water interface (0–2 cm) and in the upper 10 cm of sediments (0–10 cm), the latter of which enables comparison with other studies that are limited to 10 cm data sets (Diesing et al., 2021, 2024). The sediment accumulation rates were also used to define depths representing long-term OCBRs in sediment deposited more than 100 years ago, where excess ^{210}Pb concentrations are no longer detected. The OCARs were estimated using Equations 3 and 4 for sediment at the sediment–water interface (0–2 cm) and in the upper 10 cm of sediments (0–10 cm), respectively. OCBRs were estimated using Equation 5 for sediment deposited more than 100 years ago (40–50 cm).

Equation 3: Organic carbon accumulation rate (OCAR) calculation at the sediment–water interface (0–2 cm).

$$\text{OCAR}\left(\text{gC m}^{-2}\ \text{yr}^{-1}\right) = \text{SCD}_{\,0-2\ \text{cm}}\left(\text{gC cm}^{-3}\right) * \text{sediment accumulation rate}\left(\text{cm yr}^{-1}\right) * 10000 \quad (3)$$

Equation 4: Organic carbon accumulation rate (OCAR) calculation in the upper 10 cm of sediments (0–10 cm).

$$\text{OCAR}\left(\text{gC m}^{-2}\ \text{yr}^{-1}\right) = \text{SCD}_{\,0-10\ \text{cm}}\left(\text{gC cm}^{-3}\right) * \text{sediment accumulation rate}\left(\text{cm yr}^{-1}\right) * 10000 \quad (4)$$

Equation 5: Organic carbon burial rate (OCBR) calculation in sediment deposited more than 100 years ago (40–50 cm).

$$\text{OCBR}\left(\text{gC m}^{-2}\ \text{yr}^{-1}\right) = \text{SCD}_{\,40-50\ \text{cm}}\left(\text{gC cm}^{-3}\right) * \text{sediment accumulation rate}\left(\text{cm yr}^{-1}\right) * 10000 \quad (5)$$

2.11. Proportion of Sedimentary Organic Carbon That Is Buried

To estimate the proportion of sedimentary OC that remains buried for over 100 years across all sites, we assumed that the maximum sediment accumulation rate derived from five sediment cores was representative of the study region. For each core, we compared OC content, DBD, and SCD at the sediment–water interface (0–2 cm) and in the upper seabed (0–10 cm) with those in the 40–50 cm depth layer (100–200 years old). This comparison was used to approximate the fraction of sedimentary OC that becomes buried long-term. This approach aligns with the methods of Smeaton, Yang, and Austin (2021), which assumes that after 100 years there is no quantitative change in sedimentary OC content caused by degradation, and that the input and source of the OC has been stable over this 100-year timeframe. While it is recognized that these calculations do not consider sediment compaction and changes in sediment accumulation rate over time, they provide an initial insight into the potential long-term OC burial in the WISMB.

3. Results

3.1. Sediment Core Samples

The sediment core lengths of the 20 cores collected from the study area in the WISMB varied between 50 and 88 cm (Table S1 in Supporting Information S1). The depth profiles of the sediments (high-resolution surface sediment images and X-ray images) and the sediment variables (OC content, DBD, SCD, and relative proportions of clay, silt, and sand content) for each sediment core are in the Supporting Information (Figures S2–S21 in Supporting Information S1).

3.2. Sediment Classification

The sediment type varies spatially from mud to sandy mud across the study region, ranging from 76.96% to 96.13% within the upper 50 cm of the seabed (Table S2 in Supporting Information S1; Muir et al., 2025), and is relatively stable with sediment depth (Figures S2–S21 in Supporting Information S1). Site 6b and Site 2c were exceptions, exhibiting lower average mud contents of 71.25% and 74.83%, respectively, and having a sediment fraction more than 1,000 μm constituting 0.63%–32.41% and 0.05%–0.67% of the total sample mass, respectively.

Table 1
Average Sediment Accumulation Rates Estimated From Excess ^{210}Pb, Excess ^{210}Po, and ^{137}Cs Radioisotope Data and the Corresponding 100-Year-Old Sediment Depth

Site	Mean rate, $^{210}Pb_{xs}$ (cm yr^{-1})	Mean rate, $^{210}Po_{xs}$ (cm yr^{-1})	Mean rate, ^{137}Cs (cm yr^{-1})	Average rate (cm yr^{-1})	100-year depth (cm)
4	(0.19)	0.32	0.31	0.31 ± 0.01	31 ± 1
8	0.37	(0.26)	0.37	0.37 ± 0.00	37 ± 0
15	0.24	–	0.29	0.26 ± 0.03	26 ± 3
20	(0.35)	0.23	0.29	0.26 ± 0.04	26 ± 4
27	0.24	–	0.29	0.26 ± 0.03	26 ± 3
Average	–	–	–	0.29 ± 0.05	29 ± 5

Note. Sediment accumulation rates in parentheses were not included in the average sediment accumulation rate calculated because of high measurement uncertainty (Sites 20 and 4) and insufficient data points for regression analysis (Site 8).

3.3. Sediment Accumulation Rates

The sediment accumulation rates vary spatially across the study region, ranging from 0.26 cm yr^{-1} to 0.37 cm yr^{-1} with an average of 0.29 cm yr^{-1}, based on data from 5 cores (Table 1). Considering the maximum sediment accumulation rate of 0.37 cm yr^{-1}, the OC at a sediment depth horizon of 40–50 cm is considered buried long-term (>100 years old), representing sediment deposited between 1830 and 1915 (Table 2). Shorter-term OC accumulation is considered at the sediment–water interface (0–2 cm), whereby sediment was deposited in 2014–2022 (5–8 years old), and in the upper 10 cm of the seabed, whereby sediment was deposited in 1984–2022 (27–38 years old) (Table 2).

The average sediment accumulation rate for each sediment core is based on the rates derived from excess ^{210}Pb and ^{137}Cs radionuclides for each sediment core at three sites (Sites 8, 15, and 27) and the average rates derived from excess ^{210}Po and ^{137}Cs radionuclides for each sediment core at two sites (Sites 4 and 20), which were spatially distributed across the study region (Tables 1 and 2 and Table S3, Figures S22–S26 in Supporting Information S1; Muir et al., 2025). Average sediment accumulation rates for Sites 4 and 20 were estimated using excess ^{210}Po due to its higher sensitivity and lower measurement uncertainty compared to excess ^{210}Pb, while the average rate for Site 8 was estimated using excess ^{210}Pb due to there being insufficient excess ^{210}Po data points ($n = 3$) for regression analysis of the exponential decay curve. Sediment accumulation rates could not be estimated for Sites 14 and 21, as these had mixed radionuclide activity profiles (Figures S27–S28 in Supporting Information S1).

Overall, radionuclide activities were constant within the upper 3.5–11 cm, followed by ^{137}Cs peaks from the discharge maximum in 1975 from Sellafield nuclear facility, indicating surface mixed layers over preserved sediments. Sites 21 and 14 exhibited highly mixed sediments overlying older layers, with radionuclide activities constant in the upper 19 and 40 cm, respectively, falling below the limit of detection below these depths.

Table 2
The Average Number of Years Sediments Were Deposited Before Being Sampled (2022) and the Corresponding Sediment Deposition Date Relating to Sediment Depths (0 cm (Surface), 2, 10, 20, 30, 40, and 50 cm), Based on the Linear Sediment Accumulation Rates of 0.26–0.37 cm yr^{-1} and Average Linear Sediment Accumulation Rate of 0.29 ± 0.05 cm yr^{-1} From 5 Sediment Cores (Average Value Is in Parentheses)

Sediment depth (cm)	Years before 2022	Estimated deposition date
0	0	2022
2	5–8 (7)	2014–2017 (2015)
10	27–38 (34)	1984–1995 (1988)
20	54–77 (68)	1945–1968 (1954)
30	80–115 (102)	1907–1942 (1920)
40	107–154 (136)	1868–1915 (1886)
50	134–192 (170)	1830–1888 (1852)

3.4. Sediment Organic Carbon Contents, Dry Bulk Densities, and Sediment Organic Carbon Densities

The sedimentary OC contents, DBDs, and SCDs vary both spatially and temporally across the study region. The OC content, DBD, and SCD values ranged from 0.15% to 1.62%, 0.45 g cm^{-3} to 1.52 g cm^{-3}, and 1.30×10^{-3} gC cm^{-3} to 15.15×10^{-3} gC cm^{-3} across the full depth of sediment collected at all 20 sites (Figures S2–S21 in Supporting Information S1). The OC content and SCD generally decrease with sediment depth, whereas DBD generally increases with sediment depth. However, Site 6b, which has sandier and gravelly sediments, has the lowest OC contents, which increase with sediment depth, potentially reflecting a slightly gravelly sandy mud region, as shown by small, anomalous patches in the Seabed Sediments 250K data set (Figure 1; Table S2 in Supporting Information S1; British Geological Survey, 2024). The gravelly layers also had higher DBD uncertainty due to the challenges sampling a known volume of coarse uncompacted sediments using a U-channel. As such, data for Site 6b were

Table 3
The Range (Average ± Standard Deviation) for Organic Carbon (OC) Content (%), Sediment Dry Bulk Density (DBD, g cm^{-3}), and Sediment Organic Carbon Density (SCD, x10^{-3} gC cm^{-3}) for Sediment at the Sediment–Water Interface (0–2 cm), the Upper 10 cm (0–10 cm), and >100-Year-Old (40–50 cm), Derived From 19 Sediment Cores in the Western Irish Sea Mud Belt (WISMB)

Sediment depth (cm)	OC content (%)	DBD (g cm^{-3})	SCD (x 10^{-3} gC cm^{-3})	Mud (<63 μm, %)	$\delta^{13}C_{vPDB}$ (‰)
0–2	0.65–1.62 (1.15 ± 0.29)	0.48–1.08 (0.88 ± 0.18)	5.1–12.7 (9.8 ± 2.1)	69.04–96.48 (85.44 ± 7.56)	−25.27–(−21.92) (−22.56 ± 0.71)
0–10	0.62–1.59 (1.08 ± 0.27)	0.78–1.17 (0.99 ± 0.13)	6.7–13.8 (10.4 ± 1.6)	68.12–95.93 (85.43 ± 7.45)	−27.60–(−20.36) (−22.88 ± 1.31)
40–50	0.45–1.22 (0.72 ± 0.23)	0.91–1.52 (1.15 ± 0.15)	5.4–12.8 (8.0 ± 1.9)	68.35–96.91 (86.46 ± 7.84)	−28.67–(−22.05) (−23.04 ± 1.63)

excluded from the average data set and interpreted separately. The ranges and average values reported for OC content, DBD, SCD, and $\delta^{13}C$ below are therefore based on the results from the other 19 sediment cores (Table 3 and Table S2 in Supporting Information S1).

The OC content is generally highest in the surface sediments, ranging from 0.65% to 1.62% with an average value of 1.15% ± 0.29% at the sediment–water interface (0–2 cm), and from 0.62% to 1.59% with an average value of 1.08% ± 0.27% in the upper 10 cm (Table 3 and Table S2 in Supporting Information S1). The OC contents decrease into the sediment, with the greatest decrease generally occurring in the upper 30 cm and becoming more stable with sediment depth (Figure 2). The OC content at 40–50 cm, which is the deepest comparable depth across the 19 sediment cores and represents sediment more than 100 years old, ranges from 0.45% to 1.22% with an average value of 0.72% ± 0.23%. The proportion of OC content at 40–50 cm is 62% of the OC content at 0–2 cm and 66% of the OC content in the upper 10 cm.

Conversely, the DBD is generally lower in the surface sediments, ranging from 0.48 g cm^{-3} to 1.08 g cm^{-3} with an average value of 0.88 g cm^{-3} ± 0.18 g cm^{-3} at the sediment–water interface (0–2 cm) and from 0.78 g cm^{-3} to 1.17 g cm^{-3} with an average value of 0.99 g cm^{-3} ± 0.13 g cm^{-3} in the upper 10 cm (Table 3 and Table S2 in Supporting Information S1). The DBDs generally increase steadily in the sediment; however, at some sites, the DBD is notably lower at the sediment–water interface (0–2 cm). This uncompacted mixed surface sediment layer could be attributed to settling sediments that were resuspended in the overlying water upon retrieval of the sediment core, causing sediment decompaction and increasing the uncertainty in these surface values. The DBD at 40–50 cm ranges from 0.91 g cm^{-3} to 1.52 g cm^{-3} with an average value of 1.15 g cm^{-3} ± 0.15 g cm^{-3}. The DBD at 40–50 cm is 31% higher than the DBD at 0–2 cm and 16% higher than the DBD in the upper 10 cm.

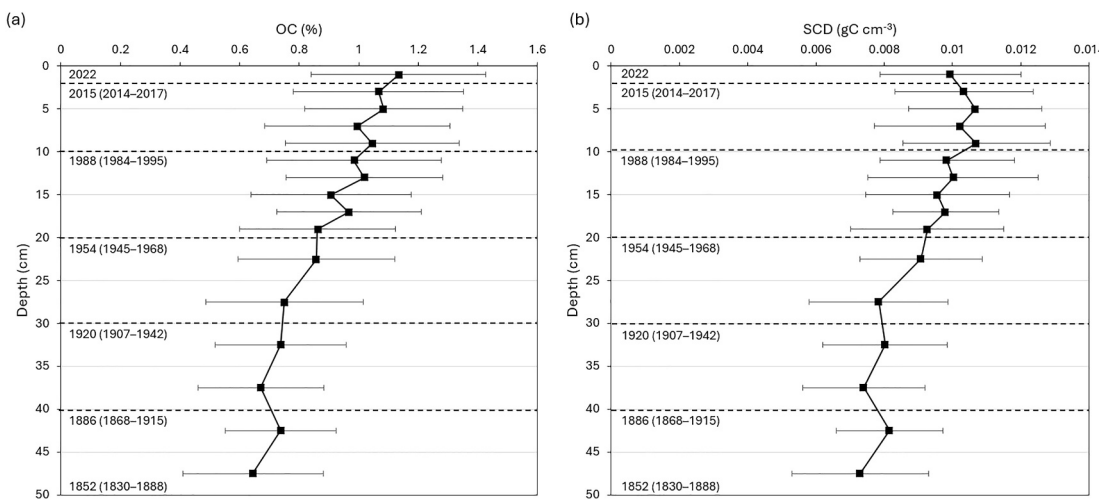

Figure 2. (a) Average sediment organic carbon content (OC, %) and (b) the average sediment organic carbon density (SCD, gC cm^{-3}) versus sediment depth (cm) for 19 sediment cores in the Western Irish Sea Mud Belt (WISMB). Error bars represent standard deviations. Dates indicate sediment deposition date estimates (average and range) at 0, 2, 10, 20, 30, 40, and 50 cm.

Table 4

Sediment OC Contents (%) at 0–2 cm and 0–10 cm (Accumulated <100 Years) and at 40–50 cm (Buried >100 Years); Sediment Accumulation Rates (cm yr^{-1}); Organic Carbon Accumulation Rates (OCARs, gC m^{-2} yr^{-1}) at 0–2 cm and 0–10 cm; Organic Carbon Burial Rates (OCBRs, gC m^{-2} yr^{-1}) at 40–50 cm; Water Depth (m, Corrected for Tidal State); and Average Mud Content (%) in the Top 50 cm, for 5 Sites Distributed Across the Study Region in the Western Irish Sea Mud Belt (WISMB)

Site ID	OC (%), 0–2 cm	OC (%), 0–10 cm	OC (%), 40–50 cm	Sediment accumulation rate (cm yr^{-1})	OCAR (gC m^{-2} yr^{-1}), 0–2 cm	OCAR (gC m^{-2} yr^{-1}), 0–10 cm	OCBR (gC m^{-2} yr^{-1}), 40–50 cm	Water depth (m)	Avg. mud content (%), 0–50 cm
Site 4	1.56	1.42	0.86	0.31	39.47	37.73	25.73	119	95.79
Site 8	1.62	1.59	0.99	0.37	36.95	51.13	33.50	116	93.45
Site 15	0.94	0.89	0.50	0.26	26.29	23.30	14.03	98	86.79
Site 27	0.78	0.78	0.47	0.26	17.09	21.90	14.35	68	78.50
Site 20	0.92	0.92	0.49	0.26	22.75	25.85	15.95	66	83.43
Average					28.51 ± 9.48	31.98 ± 12.39	20.71 ± 8.61		

Note. Table ordered by highest to lowest water depth.

The SCD reflects the spatial and temporal patterns of the OC content, but the variability is lower due to the counter effect of DBD. The influence of DBD on the temporal variability of SCD is strongest in the surface sediments (0–10 cm), where average SCD is generally stable with sediment depth (Figure 2). Overall, SCD is highest in the surface sediments, ranging from 5.1×10^{-3} gC cm^{-3} to 12.7×10^{-3} gC cm^{-3} with an average value of 9.8×10^{-3} gC cm^{-3} ± 2.1×10^{-3} gC cm^{-3} at the sediment–water interface (0–2 cm) and from 6.7×10^{-3} gC cm^{-3} to 13.8×10^{-3} gC cm^{-3} with an average value of 10.4×10^{-3} gC cm^{-3} ± 1.6×10^{-3} gC cm^{-3} in the upper 10 cm (Table 3 and Table S2 in Supporting Information S1). The lower SCD at the sediment–water interface reflects the decrease in DBD. The SCD at 40–50 cm ranges from 5.4×10^{-3} gC cm^{-3} to 12.8×10^{-3} gC cm^{-3} with an average value of 8.0×10^{-3} gC cm^{-3} ± 1.9×10^{-3} gC cm^{-3}. The proportion of SCD at 40–50 cm is 82% of the SCD at 0–2 cm, and 77% of the SCD in the upper 10 cm.

The $\delta^{13}C$ values of the sediment are relatively stable, both spatially and temporally, across the study region, with an average $\delta^{13}C$ value of −22.83‰ ± 1.62‰ in the upper 50 cm of sediment (Table 3 and Table S2 in Supporting Information S1). There are anomalous $\delta^{13}C$ values at various sediment depths, which range from −13.20 ‰ (Site 15) to −35.05 ‰ (Sites 3, 5, 6b, 10, 12b, 14, 17, 21), but these do not appear to have spatial or temporal correlations (Figures S2–S21 in Supporting Information S1).

3.5. Organic Carbon Accumulation Rates and Burial Rates

The OCARs vary spatially and temporally across the study region (Table 4; Figures S29–S33 in Supporting Information S1). The OCARs at the sediment–water interface (0–2 cm) range from 17.09 gC m^{-2} yr^{-1} to 39.47 gC m^{-2} yr^{-1}, with an average value of 28.51 ± 9.48 gC m^{-2} yr^{-1}, and the OCARs in the upper 10 cm of sediment range from 21.90 gC m^{-2} yr^{-1} to 51.13 gC m^{-2} yr^{-1}, with an average value of 31.98 ± 12.39 gC m^{-2} yr^{-1}. The OCBRs also vary spatially across the study region, whereby the OCBRs at 40–50 cm ranged from 14.03 gC m^{-2} yr^{-1} to 33.50 gC m^{-2} yr^{-1}, with an average value of 20.71 ± 8.61 gC m^{-2} yr^{-1}. Considering these results, the average OCBR is 53%–91% (average: 73% ± 15%) of the average OCAR at the sediment–water interface and 60%–68% (average: 64% ± 3%) of the average OCAR in the upper 10 cm of the seabed. The sites situated in the deepest water and with the highest mud content (Sites 4 and 8) had the highest OCARs and OCBRs, while the sites situated in the shallowest water and with the lowest mud content (Sites 15, 20, and 27) had the lowest OCARs and OCBRs (Table 4).

Extrapolating the average OCARs and OCBRs estimated for five sediment cores to the full extent of the WISMB (380,779 ha; British Geological Survey, 2024), it is estimated that the WISMB could accumulate approximately 108,556 ± 36,111 MgC yr^{-1} in the upper 2 cm of sediments deposited within the past decade, and 121,777 ± 47,186 MgC yr^{-1} in the upper 10 cm of sediments deposited from the late 1980s to the present decade. Furthermore, it is estimated that the WISMB could bury up to 78,864 ± 32,779 MgC yr^{-1} for more than 100 years in sediments that were deposited between the 1850s and 1880s.

4. Discussion

4.1. Spatial and Temporal Variability in Organic Carbon Accumulation and Burial in the Western Irish Sea Mud Belt

OCARs and OCBRs vary spatially and temporally across the WISMB study region with OCARs exceeding OCBRs. At the sediment–water interface (0–2 cm), OCARs range from 17 to 39 gC m^{-2} yr^{-1} (mean 29 gC m^{-2} yr^{-1}), and in the upper 10 cm range from 22 to 51 gC m^{-2} yr^{-1} (mean 32 gC m^{-2} yr^{-1}). Spatial variability in these rates reflects changes in sediment OC content, sediment type, and sediment accumulation rates, which are discussed in detail below. Lower OCARs at the sediment–water interface relative to the upper 10 cm reflect lower sedimentary DBDs. These are likely caused by sediment decompaction after resuspension and settling of surface sediments during sampling, as opposed to a shift toward lower density muds, which was not observed. OCBRs representing sediments more than 100 years old ranged from 14 to 34 gC m^{-2} yr^{-1} (mean 21 gC m^{-2} yr^{-1}), which are 9%–47% lower than OCARs at the sediment–water interface and 32%–40% lower than OCARs in the upper 10 cm of seabed. Relatively lower OCBRs reflect reductions in OC content and SCD with sediment depth, the causes of which are explored below.

Whilst OCARs and OCBRs are based on data from five sediment cores, they span the shallowest and deepest sites (66–119 m water depth), the least and most muddy sediments (78%–96%), and the lowest to highest OC contents (0.78%–1.59%) in the study region (spanning 66–132 m, 68%–96%, and 0.62%–1.59%, respectively). As such, they are considered representative of the broader study area, but further radionuclide dating is needed to constrain sediment accumulation rates across all sites.

The OCARs and OCBRs in the WISMB are comparable with rates from other muddy areas in temperate shelf seas, including the Helgoland Mud Area in the German Bight (4.0–57.3 gC m^{-2} yr^{-1}; Müller et al., 2025) and the West Gironde Mud Patch (WGMP) in the Bay of Biscay (28–45 gC m^{-2} yr^{-1}; Dubosq et al., 2021). While rates are comparable, these other studies are based on younger sediments buried over shorter periods of 60–65 years and shorter sediment cores (20–35 cm length), highlighting the novelty of our study in quantifying OCBRs in 50-cm-long sediments deposited over 100 years ago. These rates also align with those in the upper 10 cm of the glacial Norwegian Trough (9.29 ± 6.89 gC m^{-2} yr^{-1}; Diesing et al., 2024) and the lower rates in the coastal fjords of Scotland (35.5–110.9 gC m^{-2} yr^{-1}) (Smeaton, Yang, & Austin, 2021), highlighting the WISMB as a regional shelf sea hotspot for OC accumulation and burial.

4.1.1. Temporal Processes Regulating Long-Term Organic Carbon Burial

4.1.1.1. Organic Carbon Degradation

Differences between OCARs and OCBRs in the WISMB likely reflect OC degradation during the first 100 years of burial, as observed in the OC content and SCD profiles (Figure 2). OC content declines from 1.15% ± 0.29% (0.65%–1.62%) in the youngest 0–2 cm sediments to 1.08% ± 0.27% (0.62%–1.59%) in the upper 10 cm, and to 0.72% ± 0.23% (0.45%–1.22%) at 40–50 cm in >100-year-old sediment (Table 3). Considering this, an estimated 82% of the OC stored in the upper 2 cm ($9.8 \times 10^{-3} \pm 2.1 \times 10^{-3}$ gC cm^{-3}) and 77% in the upper 10 cm ($0.4 \times 10^{-3} \pm 1.6 \times 10^{-3}$ gC cm^{-3}) remains buried after a century ($8.0 \times 10^{-3} \pm 1.9 \times 10^{-3}$ gC cm^{-3}). These results are comparable with the burial efficiencies in Scottish fjords (77% ± 20%, Smeaton, Yang, & Austin, 2021), which compare OC content in 100-year-old sediment layers with surficial sediments.

As OC approaches 100 years of burial, below 30 cm, OC content and SCD tend toward a relatively steady state, potentially reflecting preservation of more stable refractory OC pools (Burdige, 2007). While it was not possible to assess OC content over millennia due to the limited sediment core length (max. 88 cm) and sediment accumulation rate (0.29 ± 0.03 cm yr^{-1}), the observed stability in the SCDs after 100 years suggests OC stocks in the WISMB could be stable on climate-relevant timescales (>1,000 years; Brunner et al., 2024).

A slight shift in $\delta^{13}C$ toward negative values with increasing sediment depth could indicate preferential degradation of labile marine-derived OC over time, though the subtlety of this $\delta^{13}C$ shift may highlight the degraded state of OC in the WISMB overall. These observations are consistent with conceptual models of OC remineralization and burial in marine sediments, in which labile fractions are remineralized rapidly in surface sediments, while more refractory fractions persist with depth over time (Arndt et al., 2013; Burdige, 2007; Chen et al., 2022; de Haas et al., 2002; LaRowe et al., 2020; Middelburg, 2019). In other regions, SCDs have been shown to stabilize

at shallower depths (e.g., 10–15 cm; Bakker & Helder, 1993; Hartnett et al., 1998), highlighting a need for site-specific quantification of age-resolved OC stocks to assess regional variations in long-term OC burial depths.

4.1.1.2. Sediment Compaction

While OC content continues to decrease in sediments greater than 100 years old, which could be attributed to ongoing microbial degradation deep into sediments (Bradley et al., 2022; LaRowe et al., 2020), this is offset by increasing DBD, leading to relatively stable SCD after 100 years (Figure 2 and Table S2 in Supporting Information S1). This increased DBD with sediment depth is likely to be a result of vertical auto-compaction of sediment during burial (Scourse et al., 2002); however, compaction could also have occurred during gravity coring (Skinner & McCave, 2003). Sediment compaction could impact the OCAR and OCBR estimates by underestimating sediment accumulation, overestimating DBDs, and narrowing sediment depth horizons. However, separating these potential sources of compaction was not possible due to the deep-water sampling environment and uncertainty associated with correction factor calculations.

4.1.1.3. Bioturbation

Furthermore, OC contents in the upper 10 cm of sediments increased less steeply toward the seabed surface than predicted by conceptual models (e.g., Burdige, 2007), further suggesting that the WISMB surficial sediments are relatively degraded. Sedimentary OC content may be depleted compared to incoming OC fluxes by rapid remineralization of labile OC in situ by benthic microbial and invertebrate communities, compounded by post-sampling microbial remineralization during sediment storage (Burdige, 2007; Chen et al., 2022; de Haas et al., 2002; LaRowe et al., 2020). Bioturbation may also move OC deeper into sediments leading to flatter OC content profiles and the relatively stable ^{210}Pb and ^{137}Cs activities observed in the upper 10 cm of all sediment cores (Middelburg, 2019). Consequently, OCARs may underestimate the actual OC flux to the seabed and overestimate the proportion buried long-term, likely explaining why the proportion of buried OC (77%–82%) exceeds burial efficiency estimates for other mud patches (8.5 ± 0.8%) (Wei et al., 2025).

4.1.1.4. Changes in Organic Carbon Inputs

Temporal patterns in OC content may also reflect variations in OC inputs over the past century. For example, phytoplankton biomass in the Irish Sea has increased over the past 60 years due to nutrient enrichment from terrestrial and atmospheric sources, and climatic drivers (Allen et al., 1998; Evans et al., 2003; Gowen et al., 2008). Despite this, δ^{13}C values remain at around −22‰ in the upper 50 cm of sediment, consistent with a predominantly marine signature attributable to phytoplankton-derived sources (Graves et al., 2022). Occasional significant shifts toward more negative values (down to −35‰) and less negative values (up to −13 ‰) may indicate episodic enrichment from terrestrial sources, but the absence of spatial or temporal trends suggests that long-term OC sources in the WISMB have remained broadly stable.

4.1.1.5. Changes in Sediment Accumulation Rates

Variability in sediment accumulation rates over the past century could also influence OCARs and OCBRs. While the WISMB has accumulated muddy sediments over the past several thousands of years (Ward et al., 2025), trawling-induced erosion has been detected in the southern WISMB over the past few decades (Coughlan et al., 2015), which may impact OC retention and preservation. However, agreement between excess ^{210}Pb (or excess ^{210}Po) and ^{137}Cs-derived sediment accumulation rates herein suggests net accumulation across this study region, as under erosive conditions, the ^{137}Cs activity peak would be shallower. Meanwhile, the CF–CS model used herein assumes constant accumulation through time, so shorter term changes over the past century may not be captured, adding uncertainty to the OCAR and OCBR estimates.

4.1.2. Spatial Controls on Organic Carbon Accumulation and Burial Rates

In addition to temporal changes, OCARs and OCBRs vary spatially across the WISMB, caused by variations in SCDs (Table 3) and sediment accumulation rates (Table 4). These spatial changes likely reflect variable hydrographic conditions at the edge of the WISMB that influence sediment type and seabed energy, and seasonal

variability that influences organic matter production (e.g., phytoplankton). In addition, changes in sediment supply and accumulation, as well as seabed mixing, such as proximity to rivers and anthropogenic bottom trawling, and bioturbation (e.g., *N. norvegicus*), could influence OC content and sediment accumulation.

4.1.2.1. Hydrographic Conditions

The highest OCARs and OCBRs occur at deeper, muddier sites across the WISMB, where sediment accumulation rates and OC content are greatest (Table 4). These patterns align with spatially variable hydrographic conditions, which influence the distribution and retention of fine-grained muddy sediment (Belderson, 1964; Coughlan et al., 2021; Williams et al., 2019). Reduced bed shear stress in deeper areas promotes mud retention, increases OC adsorption, reduces oxygen exposure time, and enhances organic matter preservation compared with shallower sandier margins (Burdige, 2007; Müller et al., 2025). Higher sedimentary OC content in the deeper regions relative to shallower areas has also been observed previously in the southern WISMB (O'Reilly et al., 2014).

Seasonal stratification and summer gyre formation also influence the phytoplankton production, transport, and fate in the WISMB. Phytoplankton biomass tends to be higher in well-mixed waters than in stratified regions, while copepod grazing is a key pathway for organic matter remineralization, particularly during seasonal blooms (O'Reilly et al., 2014). Marine OC inputs may therefore be spatially varied, reflecting the transition from mixed to stratified waters and from sandy to muddy sediments (O'Reilly et al., 2014). Freshwater discharges from rivers along Ireland's east coast provide the primary source of terrestrial OC to the Western Irish Sea (O'Reilly et al., 2014), but given the relatively small size of the study area and the similar distances to major river inputs at all sites, terrestrial OC supply across the northeastern WISMB is likely to be broadly comparable. Additional OC source characterization (e.g., $\delta^{15}N$, C:N), building on $\delta^{13}C$ values, could help clarify how source variations influence both short- and long-term OC storage (Graves et al., 2022).

4.1.2.2. Sediment Supply and Seabed Disturbance

Although the five dated cores are expected to be broadly representative of the study region, sediment accumulation rates in the northeastern WISMB (0.26–0.37 cm yr^{-1}) are notably lower than those previously reported in the southwest, where modern rates reach 0.8–1.0 cm yr^{-1} and historic rates 2.1–2.7 cm yr^{-1} (Coughlan et al., 2015). Such differences could reflect multiple interacting factors, including spatial variations in riverine sediment supply (Müller et al., 2025), sediment resuspension and erosion linked to bottom trawling (Martín, Puig, Palanques, & Giamportone, 2014), and differences in sediment mobilization, settling, and erosion associated with benthic boundary layer thickness within the Western Irish Sea gyre (Hill et al., 1997; Williams et al., 2019). Rivers along Ireland's east coast likely elevate terrestrial sediment fluxes to the southern WISMB (O'Reilly et al., 2014), while the erosive impacts of higher fishing pressure in the south (European Marine Observation and Data Network, 2024) may be partially offset by the narrow benthic boundary layer that can trap and retain sediments (Hill et al., 1997; Williams et al., 2019). Although Coughlan et al. (2015) suggest that erosion may have removed the top 20–50 cm of surficial sediment in the southern WISMB, corroboration between ^{137}Cs and excess ^{210}Pb dating herein indicates sediment retention in the northeastern study region. Collectively, these findings highlight the need for WISMB-wide sediment analyses to better resolve spatial variability in OCARs and OCBRs across this broader region.

Seabed mixing in parts of the WISMB also reflects spatially variable sediment accumulation in the study region. Two cores (Sites 14 and 21) exhibited constant radionuclide profiles with sediment depth, no ^{137}Cs peak, and relatively stable OC content with depth (Figures S11, S18, S27, and S28 in Supporting Information S1), indicating substantial seabed mixing and inhibiting sediment accumulation rate estimates at these sites. Notably, radionuclide activities (^{210}Pb, ^{137}Cs, ^{241}Am) and OC contents at these mixed sites were comparable to those at other locations, suggesting that mixing may flatten profiles without necessarily depleting OC (Middelburg, 2019). This could reflect rapid accumulation or burial of fresh OC deposits, mixing of fresher and older sediment layers, or local depositional variability.

As one of the most heavily trawled shelf sea regions globally and with a dense population of *Nephrops norvegicus* (Norway lobster), the WISMB is subject to high levels of sediment reworking through bioturbation and bottom trawl penetration. Post-depositional disturbance can accelerate OC remineralization leading to reduced sedimentary OC storage (Song et al., 2022), resulting in depleted and/or constant radionuclide and OC profiles with

depth (Martín, Puig, Masqué, et al., 2014). Evidence of surface mixing was observed in the upper 10 cm of all cores, where relatively stable or fluctuating ^{210}Pb and ^{137}Cs activities and lower than expected OC contents (relative to conceptual models; Burdige, 2007) matched patterns reported for other mud patches (Dubosq et al., 2021) and trawled areas (Paradis et al., 2019). Additional artifacts may arise from gravity coring itself, as resuspended material settling at the sediment–water interface can reduce surficial DBDs and underestimate SCDs and OCARs across the study region. X-ray radiographs showed evidence of mixing to 40 cm in most cores, suggesting widespread sediment mixing across the study region. Future work should therefore examine the combined effects of bottom trawling, *N. norvegicus* bioturbation, waves, and tidal currents on sedimentary OC content in the WISMB, building on insights from other muddy environments (Martín, Puig, Palanques, & Giamportone, 2014; Paradis et al., 2019; van de Velde et al., 2018; Zhang et al., 2024), to assess their influence on OCARs and OCBRs, and investigate OC reactivity to quantify the stability of OC in deeper sediments.

4.1.3. Upscaling and Future Work to Constrain Spatial Variability

When upscaled to the full WISMB area (380,779 ha), OC accumulation was estimated to be 109,000 MgC yr^{-1} in sediments deposited within the past decade (0–2 cm) and 122,000 MgC yr^{-1} in sediments deposited since the late 1980s (0–10 cm), while OC burial was estimated to be 79,000 MgC yr^{-1} in sediments deposited 100–200 years ago (40–50 cm). These rates are comparable to the Scottish fjords (84,000 MgC yr^{-1} over 260,800 ha; Smeaton, Yang, & Austin, 2021) and exceed the WGMP (11,760–18,900 MgC yr^{-1} over 42,000 ha; Dubosq et al., 2021). The study area spans a transition from shallower sandy seabed to deeper muddy seabed at the WISMB edge, where OC content increases with mud content and sediment accumulation rates are lower than previous estimates for the southwest WISMB (Coughlan et al., 2015). As a result, upscaling our results could overestimate OC burial in coarser sediments and underestimate it in finer sediments.

Site 6b contained notably coarser sediments, including a gravel layer, consistent with the British Geological Survey classifications of slightly gravelly mud and slightly gravelly sandy mud in the region (Figure 1), and exhibits increasing OC content with depth. Although coarser sediments are a minor component of the WISMB, characterizing and incorporating them could improve OCAR and OCBR estimates. Further research across the whole WISMB is needed to quantify the spatial variability in OC stocks, as well as OCARs and OCBRs, and to assess how sediment type, OC inputs, and sediment mixing shape carbon dynamics in the WISMB.

5. Conclusions

This study provides the first age-resolved estimates of OC accumulation and burial over the past two centuries in the upper 50 cm of the WISMB, using empirical depth- and age-resolved OC content and sediment accumulation rates derived from radionuclide dating. Results show a marked decline in OC content within the first 100 years after deposition, followed by relatively stable stocks in older sediments, underscoring the importance of age-resolved analyses for distinguishing short-term accumulation from long-term burial. Despite spatial variability across this marginal study area, OC accumulation and burial rates were comparable to other temperate depositional shelf regions, including mud patches, fjords, and glacial troughs, with muddier, deeper sediments exhibiting the highest rates. These findings highlight how limiting estimates to surface sediments (e.g., top 10 cm) can overstate their climate mitigation potential if OC degrades with depth. Overall, this study demonstrates that empirical age-resolved measurements refine estimates of long-term OC burial and improve understanding of the role of muddy shelf seas in climate regulation, while emphasizing the need for further research to upscale estimates across the wider WISMB and assess the influence of spatial and temporal variability in OC inputs and sediment dynamics.

Conflict of Interest

The authors declare no conflicts of interest relevant to this study.

Data Availability Statement

The sedimentary data used for the analyses in the study are available at PANGAEA® Data Publisher (https://doi.org/10.1594/PANGAEA.983345).

Acknowledgments
The authors acknowledge financial support for this research from the Department of Environment, Food and Agriculture (DEFA), Isle of Man Government. The authors thank Dr Stuart Jenkins from Bangor University and Dr Jack Emmerson and Dr Kev Kennington from DEFA for helpful research discussions as part of the Manx Blue Carbon Working Group. The authors also thank the crew of the Barrule fisheries enforcement vessel for their help in collecting sediment cores. HM additionally thanks Dr James Hunt from the National Oceanography Centre and Dr Hachem Kassem from the University of Southampton for technical help with particle size analysis; Dr Sargent Bray and Bastian Hambach from the University of Southampton for access to their freeze dryer; Dr Pawel Gaca from the University of Southampton for sample preparation training for alpha spectrometry; the team at the British Ocean Sediment Core Research Facility (BOSCORF) for supporting sediment core processing and the generation of X-radiographs and high-resolution images (MSCL-CIS); and summer student Beth Archer (University of Exeter) for their help with sample preparation.

References

Allen, J. R., Slinn, D. J., Shummon, T. M., Hurtnoll, R. G., & Hawkins, S. J. (1998). Evidence for eutrophication of the Irish Sea over four decades. *Limnology & Oceanography*, *43*(8), 1970–1974. https://doi.org/10.4319/lo.1998.43.8.1970

Aller, R. C. (1994). Bioturbation and remineralization of sedimentary organic matter: Effects of redox oscillation. *Chemical Geology*, *114*(3), 331–345. https://doi.org/10.1016/0009-2541(94)90062-0

Appleby, P. G., & Oldfield, F. (1978). The calculation of lead-210 dates assuming a constant rate of supply of unsupported 210Pb to the sediment. *Catena*, *5*(1), 1–8. https://doi.org/10.1016/S0341-8162(78)80002-2

Arndt, S., Jørgensen, B. B., LaRowe, D. E., Middelburg, J. J., Pancost, R. D., & Regnier, P. (2013). Quantifying the degradation of organic matter in marine sediments: A review and synthesis. *Earth-Science Reviews*, *123*, 53–86. https://doi.org/10.1016/j.earscirev.2013.02.008

Atwood, T. B., Witt, A., Mayorga, J., Hammill, E., & Sala, E. (2020). Global patterns in marine sediment carbon stocks. *Frontiers in Marine Science*, *7*(165), 1–9. https://doi.org/10.3389/fmars.2020.00165

Bakker, J. F., & Helder, W. (1993). Skagerrak (northeastern North Sea) oxygen microprofiles and porewater chemistry in sediments. *Marine Geology*, *111*(3–4), 299–321. https://doi.org/10.1016/00253227(93)90137-K

Belderson, R. H. (1964). Holocene sedimentation in the western half of the Irish Sea. *Marine Geology*, *2*(1), 147–163. https://doi.org/10.1016/0025-3227(64)90032-5

Bowers, D. G., Roberts, E. M., White, M., & Moate, B. D. (2013). Water masses, mixing, and the flow of dissolved organic carbon through the Irish Sea. *Continental Shelf Research*, *58*(5), 12–20. https://doi.org/10.1016/j.csr.2013.02.007

Bradley, J. A., Hülse, D., LaRowe, D. E., & Arndt, S. (2022). Transfer efficiency of organic carbon in marine sediments. *Nature Communications*, *13*(1), 7297. https://doi.org/10.1038/s41467-022-35112-9

British Geological Survey. (2024). Seabed sediments 250K [Dataset]. Retrieved from https://www.bgs.ac.uk/datasets/marine-sediments-250k/

Brunner, C., Hausfather, Z., & Knutti, R. (2024). Durability of carbon dioxide removal is critical for Paris climate goals. *Communications Earth & Environment*, *13*(1), 645. https://doi.org/10.1038/s43247-024-01808-7

Burdige, D. J. (2007). Preservation of organic matter in marine sediments: Controls, mechanisms, and an imbalance in sediment organic carbon budgets? *Chemical Reviews*, *107*(2), 467–485. https://doi.org/10.1021/cr050347q

Burrows, M. T., O'Dell, A., Tillin, H., Grundy, S., Sugden, H., Moore, P., et al. (2024). The United Kingdom's blue carbon inventory: Assessment of marine carbon storage and sequestration potential in UK Seas (including within marine protected areas). A Report to The Wildlife Trusts, WWF and the RSPB. Scottish Association for Marine Science, Oban.

Chen, Z., Nie, T., Zhao, X., Li, J., Yang, B., Cui, D., et al. (2022). Organic carbon remineralization rate in global marine sediments: A review. *Regional Studies in Marine Science*, *49*, 102112. https://doi.org/10.1016/j.rsma.2021.102112

Coughlan, M., Guerrini, M., Creane, S., O'Shea, M., Ward, S. L., Van Landeghem, K. J. J., et al. (2021). A new seabed mobility index for the Irish Sea: Modelling seabed shear stress and classifying sediment mobilisation to help predict erosion, deposition, and sediment distribution. *Continental Shelf Research*, *229*, 104574. https://doi.org/10.1016/j.csr.2021.104574

Coughlan, M., Wheeler, A. J., Dorschel, B., Lordan, C., Boer, W., van Gaever, P., et al. (2015). Record of anthropogenic impact on the Western Irish Sea mud belt. *Anthropocene*, *9*, 56–69. https://doi.org/10.1016/j.ancene.2015.06.001

de Haas, H., van Weering, T. C. E., & de Stigter, H. (2002). Organic carbon in shelf seas: Sinks or sources, processes and products. *Continental Shelf Research*, *22*(5), 691–717. https://doi.org/10.1016/S0278-4343(01)00093-0

Diesing, M., Paradis, S., Jensen, H., Thorsnes, T., Bjarnadóttir, L. R., & Knies, J. (2024). Glacial troughs as centres of organic carbon accumulation on the Norwegian continental margin. *Communications Earth & Environment*, *5*(1), 327. https://doi.org/10.1038/s43247-024-01502-8

Diesing, M., Thorsnes, T., & Bjarnadóttir, L. R. (2021). Organic carbon densities and accumulation rates in surface sediments of the North Sea and Skagerrak. *Biogeosciences*, *18*(6), 2139–2160. https://doi.org/10.5194/bg-18-2139-2021

Dubosq, N., Schmidt, S., Walsh, J. P., Grémare, A., Gillet, H., Lebleu, P., et al. (2021). A first assessment of organic carbon burial in the West Gironde Mud Patch (Bay of Biscay). *Continental Shelf Research*, *221*, 104419. https://doi.org/10.1016/j.csr.2021.104419

European Marine Observation and Data Network. (2024). Average surface swept area ratio 2019–2022, Celtic Seas. Retrieved from https://emodnet.ec.europa.eu/geoviewer/

Evans, G. L., Williams, P. L. B., & Mitchelson-Jacob, E. G. (2003). Physical and anthropogenic effects on observed long-term nutrient changes in the Irish Sea. *Estuarine, Coastal and Shelf Science*, *57*(5), 1159–1168. https://doi.org/10.1016/S0272-7714(03)00056-8

Folk, R. L. (1954). The distinction between grain size and mineral composition in sedimentary-rock nomenclature. *The Journal of Geology*, *62*(4), 344–359. https://doi.org/10.1086/626171

GEBCO Compilation Group. (2024). GEBCO 2024 Grid [Dataset]. *General Bathymetric Chart of the Oceans*. https://doi.org/10.5285/1c44ce99-0a0d-5f4f-e063-7086abc0ea0f

Gowen, R. J., Tett, P., Kennington, K., Mills, D. K., Shammon, T. M., Stewart, B. M., et al. (2008). The Irish Sea: Is it eutrophic? *Estuarine, Coastal and Shelf Science*, *76*(2), 239–254. https://doi.org/10.1016/j.ecss.2007.07.005

Graves, C. A., Benson, L., Aldridge, J., Austin, W. E. N., Dal Molin, F., Fonseca, V. G., et al. (2022). Sedimentary carbon on the continental shelf: Emerging capabilities and research priorities for Blue Carbon. *Frontiers in Marine Science*, *9*, 926215. https://doi.org/10.3389/fmars.2022.926215

Gray, J., Jones, S. R., & Smith, A. D. (1995). Discharges to the environment from the Sellafield site, 1951-1992. *Journal of Radiological Protection*, *15*(2), 99–131. https://doi.org/10.1088/0952-4746/15/2/001

Hartnett, H. E., Keil, R. G., Hedges, J. I., & Devol, A. H. (1998). Influence of oxygen exposure time on organic carbon preservation in continental margin sediments. *Nature*, *391*(6667), 572–575. https://doi.org/10.1038/35351

Hill, A. E., Brown, J., & Fernand, L. (1997). The summer gyre in the Western Irish Sea: Shelf sea paradigms and management implications. *Estuarine, Coastal and Shelf Science*, *44*, 83–95. https://doi.org/10.1016/S0272-7714(97)80010-8

Hill, J. M. (2007). *Structure and flow of carbon and nitrogen to the western Irish Sea Nephrops norvegicus fishery: A stable isotope approach* (Thesis, Doctor of Philosophy). University of London. Retrieved from https://qmro.qmul.ac.uk/jspui/handle/123456789/1483

Howard, S. H. J., Isensee, K., Pidgeon, E., & Telszewski, M. (2014). *Coastal Blue Carbon: Methods for assessing carbon stocks and emissions factors in mangroves, tidal salt marshes, and seagrass meadows*. Conservation International, Intergovernmental Oceanographic Commission of UNESCO, International Union for Conservation of Nature.

Hu, L., Shi, X., Bai, Y., Qiao, S., Li, L., Yu, Y., et al. (2016). Recent organic carbon sequestration in the shelf sediments of the Bohai Sea and Yellow Sea, China. *Journal of Marine Systems*, *155*, 50–58. https://doi.org/10.1016/j.jmarsys.2015.10.018

Johannessen, S. C. (2023). How to quantify blue carbon sequestration rates in seagrass meadow sediment: Geochemical method and trouble-shooting. *Carbon Footprints*, *2*(4), 21. https://doi.org/10.20517/cf.2023.37

Kershaw, P. J. (1986). Radiocarbon dating of Irish Sea sediments. *Estuarine, Coastal and Shelf Science*, *23*(3), 295–303. https://doi.org/10.1016/0272-7714(86)90029-6

Kristensen, E., Flindt, M. R., & Quintana, C. O. (2025). Predicting climate mitigation through carbon burial in blue carbon Ecosystems—Challenges and pitfalls. *Global Change Biology*, *31*(1), e70022. https://doi.org/10.1111/gcb.70022

LaRowe, D. E., Arndt, S., Bradley, J. A., Estes, E. R., Hoarfrost, A., Lang, S. Q., et al. (2020). The fate of organic carbon in marine sediments - New insights from recent data and analysis. *Earth-Science Reviews*, *204*, 103146. https://doi.org/10.1016/j.earscirev.2020.103146

Martín, J., Puig, P., Masqué, P., Palanques, A., & Sánchez-Gómez, A. (2014). Impact of bottom trawling on deep-sea sediment properties along the flanks of a submarine canyon. *PLoS One*, *9*(8), e104536. https://doi.org/10.1371/journal.pone.0104536

Martín, J., Puig, P., Palanques, A., & Giamportone, A. (2014). Commercial bottom trawling as a driver of sediment dynamics and deep seascape evolution in the Anthropocene. *Anthropocene*, *7*, 1–15. https://doi.org/10.1016/j.ancene.2015.01.002

Mason, C. (2022). *NMBAQC's best practice guidance Particle Size Analysis (PSA) for supporting biological analysis*. CEFAS.

Mathis, M., Lacroix, F., Hagemann, S., Nielsen, D. M., Ilyina, T., & Schrum, C. (2024). Enhanced CO_2 uptake of the coastal ocean is dominated by biological carbon fixation. *Nature Climate Change*, *14*(4), 373–379. https://doi.org/10.1038/s41558-024-01956-w

Middelburg, J. J. (2019). In *Marine carbon biogeochemistry: A primer for Earth system scientists*. Springer International Publishing. https://doi.org/10.1007/978-3-030-10822-9_4

Muir, H. C., Reading, D. G., Warwick, P. E., Peel, K., & Evans, C. (2025). Sediment core data (organic carbon, dry bulk density, grain size, radionuclide) from the Western Irish Sea Mud Belt June 2022 [Dataset bundled publication]. *PANGAEA*. https://doi.org/10.1594/PANGAEA.983345

Müller, D., Liu, B., Geibert, W., Holtappels, M., Sander, L., Miramontes, E., et al. (2025). Depositional controls and budget of organic carbon burial in fine-grained sediments of the North Sea – The Helgoland Mud Area as a natural laboratory. *Biogeosciences*, *22*(11), 2541–2567. https://doi.org/10.5194/bg-22-2541-2025

O'Reilly, S. S., Szpak, M. T., Flanagan, P. V., Monteys, X., Murphy, B. T., Jordan, S. F., et al. (2014). Biomarkers reveal the effects of hydrography on the sources and fate of marine and terrestrial organic matter in the western Irish Sea. *Estuarine, Coastal and Shelf Science*, *136*, 157–171. https://doi.org/10.1016/j.ecss.2013.11.002

Paradis, S., Pusceddu, A., Masqué, P., Puig, P., Moccia, D., Russo, T., & Lo Iacono, C. (2019). Organic matter contents and degradation in a highly trawled area during fresh particle inputs (Gulf of Castellammare, southwestern Mediterranean). *Biogeosciences*, *16*(21), 4307–4320. https://doi.org/10.5194/bg-16-4307-2019

Ray, D., Leary, P., Livens, F., Gray, N., Morris, K., Law, K. A., et al. (2020). Controls on anthropogenic radionuclide distribution in the Sellafield-impacted Eastern Irish Sea. *Science of the Total Environment*, *743*, 140765. https://doi.org/10.1016/j.scitotenv.2020.140765

Sanders, C. J., Smoak, J. M., Naidu, A. S., Sanders, L. M., & Patchineelam, S. R. (2010). Organic carbon burial in a mangrove forest, margin and intertidal mud flat Estuarine. *Coastal and Shelf Science*, *90*(3), 168–172. https://doi.org/10.1016/j.ecss.2010.08.013

Scourse, J. D., Austin, W. E. N., Long, B. T., Assinder, D. J., & Huws, D. (2002). Holocene evolution of seasonal stratification in the Celtic Sea: Refined age model, mixing depths and foraminiferal stratigraphy. *Marine Geology*, *191*(3–4), 119–145. https://doi.org/10.1016/S0025-3227(02)00528-5

Skinner, L. C., & McCave, I. N. (2003). Analysis and modelling of gravity- and piston coring based on soil mechanics. *Marine Geology*, *199*(1–2), 181–204. https://doi.org/10.1016/s0025-3227(03)00127-0

Smeaton, C., Hunt, C. A., Turrell, W. R., & Austin, W. E. N. (2021a). Marine sedimentary carbon stocks of the United Kingdom's exclusive economic zone. *Frontiers in Earth Science*, *9*, 593324. https://doi.org/10.3389/feart.2021.593324

Smeaton, C., Yang, H., & Austin, W. E. N. (2021). Carbon burial in the mid-latitude fjords of Scotland. *Marine Geology*, *441*, 106618. https://doi.org/10.1016/j.margeo.2021.106618

Song, S., Santos, I. R., Yu, H., Wang, F., Burnett, W. C., Bianchi, T. S., et al. (2022). A global assessment of the mixed layer in coastal sediments and implications for carbon storage. *Nature Communications*, *13*(1), 4903. https://doi.org/10.1038/s41467-022-32650-0

Udden, J. A. (1914). Mechanical composition of clastic sediments. *Geological Society of America Bulletin*, *25*(1), 655–754. https://doi.org/10.1130/GSAB-25-655

van de Velde, S., Van Lancker, V., Hidalgo-Martinez, S., Berelson, W. M., & Meysman, F. J. R. (2018). Anthropogenic disturbance keeps the coastal seafloor biogeochemistry in a transient state. *Scientific Reports*, *8*(1), 5582. https://doi.org/10.1038/s41598-018-23925-y

Ward, S. L., Bradley, S. L., Roseby, Z. A., Wilmes, S.-B., Vosper, D. F., Roberts, C. M., & Scourse, J. D. (2025). The role of long-term hydrodynamic evolution in the accumulation and preservation of organic carbon-rich shelf sea deposits. *Journal of Geophysical Research: Oceans*, *130*(4), e2024JC022092. https://doi.org/10.1029/2024JC022092

Wei, B., Müller, D., Kusch, S., Niu, L., Hefter, J., Sander, L., et al. (2025). Twice the global average carbon burial efficiency in the Helgoland Mud Area of the North Sea: Insights into carbon sequestration in small-size depocenters on sand-dominated shelves. *Chemical Geology*, *681*, 122712. https://doi.org/10.1016/j.chemgeo.2025.122712

Wentworth, C. K. (1922). A scale of grade and class terms for clastic sediments. *The Journal of Geology*, *30*(5), 377–392. https://doi.org/10.1086/622910

Wilkinson, G. M., Besterman, A., Buelo, C., Gephart, J., & Pace, M. L. (2018). A synthesis of modern organic carbon accumulation rates in coastal and aquatic inland ecosystems. *Scientific Reports*, *8*(1), 15736. https://doi.org/10.1038/s41598-018-34126-y

Williams, M. E., Amoudry, L. O., Brown, J. M., & Thompson, C. E. L. (2019). Fine particle retention and deposition in regions of cyclonic tidal current rotation. *Marine Geology*, *410*, 122–134. https://doi.org/10.1016/j.margeo.2019.01.006

Williamson, P., & Gattuso, J.-P. (2022). Carbon removal using coastal blue carbon ecosystems is uncertain and unreliable, with questionable climatic cost-effectiveness. *Frontiers in Climate*, *4*, 853666. https://doi.org/10.3389/fclim.2022.853666

Zhang, W., Porz, L., Yilmaz, R., Wallmann, K., Spiegel, T., Neumann, A., et al. (2024). Long-term carbon storage in shelf sea sediments reduced by intensive bottom trawling. *Nature Geoscience*, *17*(12), 1268–1276. https://doi.org/10.1038/s41561-024-01581-4

References From the Supporting Information

European Marine Observation and Data Network. (2022). Bathymetric contours (version 2022) [Dataset]. *EMODnet Bathymetry*. Retrieved from https://emodnet.ec.europa.eu/geoviewer/